# Block Copolymers in Electric Fields: A Comparison of Single-Mode and Self-Consistent-Field Approximations

**Yoav Tsori\***

*Department of Chemical Engineering, Ben Gurion University, P.O. Box 653, Beer Sheva 84105, Israel*

**David Andelman**

*School of Physics and Astronomy, Raymond and Beverly Sackler Faculty of Exact Sciences, Tel Aviv University, Ramat Aviv 69978, Tel Aviv, Israel*

**Chin-Yet Lin and M. Schick**

*Physics Department, Box 351560, University of Washington, Seattle, Washington 98195*

ABSTRACT: We compare two theoretical approaches to diblock copolymer melts in an external electric field. The first is a relatively simple analytic expansion in the copolymer composition and includes the full electrostatic contribution consistent with that expansion. It is valid close to the order−disorder transition point, the weak segregation limit. The second employs self-consistent-field (SCF) theory and includes the full electrostatic contribution to the free energy at any copolymer segregation. It is more accurate but computationally more intensive. Motivated by recent experiments, we explore a section of the phase diagram in the three-dimensional parameter space of the block architecture, the interaction parameter, and the external electric field. The relative stability of the lamellar, hexagonal, and distorted body-centered-cubic (bcc) phases is compared within the two models. As function of an increasing electric field, the distorted bcc region in the phase diagram shrinks and disappears above a triple point, at which the lamellar, hexagonal, and distorted bcc phases coexist. We examine the deformation of the bcc phase under the influence of the external field. While the elongation of the spheres is larger in the one-mode expansion than that predicted by the full SCF theory, the general features of the schemes are in satisfactory agreement. This indicates the general utility of the simple theory for exploratory calculations.

## I. Introduction

Block copolymers (BCP) consist of several chemically distinct subchains. They are interesting not only as a model system for self-assembly but also for their chemical versatility and affordability which have enabled their use in applications such as photonic waveguides,[1] tough plastics,[2,3] ordered arrays of nanowires,[4] etc. At a given chemical architecture and temperature, there is one thermodynamically stable mesophase, with typical length scales comparable to the chain size (∼10−500 nm). However, the material is rarely perfectly ordered, but rather is composed of many randomly oriented grains of size ∼1 $\mu$m. This has an adverse effect on nanotechnological applications.

A useful way to achieve improved long-range order is to subject the BCP sample above its glass transition to an external electric field $\mathbf{E}_0$. Because of the coupling between the field and the spatially varying dielectric constant $\kappa(\mathbf{r})$, there is a preferred orientation of the grains with respect to the field.[5−14] It has been shown by Amundson et al.[5,6] that the electrostatic free energy penalty associated with dielectric interfaces which are not parallel to the electric field direction is the driving force for structures to reorient so that their interfaces are parallel to the field ($\nabla\kappa(\mathbf{r})$ perpendicular to $\mathbf{E}_0$). While the free energy penalty can be eliminated by this reorientation of lamellae and cylinders, it cannot be eliminated in the body-centered-cubic (bcc) phase but only reduced by distorting the bcc spheres. Thus, the free energy of this distorted bcc phase, whose symmetry is reduced to $R\bar{3}m$, increases with respect to the full disordered liquid (dis), lamellar (lam), and hexagonal (hex) phases,[12] a circumstance

which can bring about a phase transition. The effect of the electric field on the BCP morphology has been substantially accounted for recently[15] by incorporating the electrostatic Maxwell equations in the full set of self-consistent-field (SCF) equations, which permits calculation of the phase diagram at arbitrary degrees of segregation.

In this paper we compare two theoretical approaches to such a system: the aforementioned SCF study and a simple analytical approximation consisting of a Ginzburg−Landau expansion of the free energy,[16] valid only close to the order−disorder temperature (ODT). It is assumed that the polymers under consideration here are ion-free, so the effect of mobile dissociated ions, which can be dramatic in some systems,[12−14] can be ignored.

The paper is organized as follows. In section 2 we present the free energy model which includes the electrostatic energy of the BCP in the field. In section 3 we calculate the way in which an initial mesophase deforms under the influence of the field and also find the relative stability of the competing phases. A comparison is made with the results of the SCF model. Section 4 contains a brief conclusion.

## II. Model

Although the effect we consider here is generic to any multiblock BCP melts, we will restrict the discussion in this paper to the simplest A/B diblock copolymer, where a spatial variation of the relative A/B monomer concentration yields a spatial dependence of the dielectric constant and, hence, of the response to an external electric field.

We also assume for simplicity that the A monomeric volume is equal to the B one. Then the volume fraction of the A

monomers, $f$ ($0 \leq f \leq 1$), is equal to its molar fraction. The order parameter $\phi(\mathbf{r})$ is defined as the local deviation of the A-monomer fraction $\phi_A(\mathbf{r})$ from its average value: $\phi(\mathbf{r}) = \phi_A(\mathbf{r}) - f$. From an incompressibility condition of the melt we also have at each point $\mathbf{r}$, $\phi_B(\mathbf{r}) = 1 - \phi_A(\mathbf{r})$. In the absence of any external electric fields, the bulk BCP free energy per polymer chain, $F_b$, in units of $k_B T$, can be written as a functional of the order parameter, $\phi(\mathbf{r})$. One way of generating a simple analytical expansion in the order parameter relies on a Ginzburg−Landau-like free energy, which can be justified close to the order−disorder point (ODT)[16−18] and is repeated here without further justifications:

$$F_b = \frac{1}{\Omega} \int \left\{ \frac{1}{2}\tau\phi^2 + \frac{1}{2}h(\nabla^2\phi + q_0^2\phi)^2 + \frac{\lambda}{6}\phi^3 + \frac{u}{24}\phi^4 \right\} d^3r \quad (1)$$

where $\Omega$ is the system volume and

$$\tau = \frac{2N(\chi_s - \chi)}{c^2}, \quad q_0 \sim 1/R_g = \left(\frac{1}{6}Nb^2\right)^{-1/2}, \quad h = \frac{3}{2}\frac{R_g^2}{q_0^2} \quad (2)$$

$b$ is the Kuhn length, $R_g$ is the radius of gyration, $\chi$ is the Flory parameter, $N = N_A + N_B$ is the total chain polymerization index, $N\chi_s$ is the spinodal value[16] of $\chi N$, $c$ is a constant of order 1, and $\lambda$ and $u$ are functions of $f$ as in refs 16−18. The phase diagram in the ($f,\chi N$) plane, as derived from the free energy, eq 1, is symmetric with respect to exchange of $f$ and $1 - f$. For small values of $\chi \sim 1/T$, the melt is disordered: $\phi(\mathbf{r}) = 0$ is constant. For $\chi N$ larger than the ODT value of $\simeq 10.5$ and for nearly symmetric BCP composition ($f \approx 1/2$), the lamellar phase is the most stable. As $|f - 1/2|$ increases, the stable phases are doubly connected gyroid, hexagonal, and bcc phases.[16,17,19]

Let us now consider a BCP slab placed in an external electric field, $\mathbf{E}_0$. The free energy per polymer chain, again in units of $k_B T$, is $F_{tot} = F_b + F_{es}$, where the electrostatic energy contribution $F_{es}$ is given by the integral over the square of the local electric field $E(\mathbf{r}) = -\nabla\psi$

$$F_{es} = -\frac{1}{2}\frac{\epsilon_0 \upsilon_p}{k_B T \Omega} \int \kappa(\mathbf{r})[\nabla\psi(\mathbf{r})]^2 \, d^3r \quad (3)$$

Here $\epsilon_0$ is the vacuum permittivity, $\kappa(\mathbf{r})$ is the local dielectric constant, $\upsilon_p$ is the volume per chain, and $\psi$ is the electrostatic potential obeying the proper boundary conditions on the electrodes. We note that the variation of $F_{es}$ with respect to $\psi$ yields

$$\nabla \cdot (\epsilon_0 \kappa(\mathbf{r})\nabla\psi) = 0 \quad (4)$$

which is the usual Maxwell equation $\nabla \cdot \mathbf{D} = 0$ for the displacement field $\mathbf{D} = \epsilon_0 \kappa \mathbf{E}$. We consider a simple geometry of a BCP slab filling the gap between two parallel and flat electrodes separated by a distance $d$ and potential difference $V$. Even when a nonhomogeneous dielectric material like a BCP fills the gap between the two electrodes, the spatially averaged electric field in between the electrodes $\langle\mathbf{E}\rangle$ is constrained to be $E_0 = V/d$. The local field $\mathbf{E}(\mathbf{r})$ differs from its average due to the nonuniformity of the dielectric constant, since $\kappa = \kappa(\phi)$ depends on the local concentration $\phi(\mathbf{r})$ through a constitutive equation. In this paper we assume for simplicity a linear constitutive relation

$$\kappa(\mathbf{r}) = \langle\kappa\rangle + \phi(\mathbf{r})\Delta\kappa, \quad \Delta\kappa \equiv \kappa_A - \kappa_B,$$
$$\langle\kappa\rangle = f\kappa_A + (1 - f)\kappa_B \quad (5)$$

where throughout this paper we use $\kappa_A = 6.0$ and $\kappa_B = 2.5$,

thus modeling an A/B diblock copolymer in which the A block is poly(methyl methacrylate) (PMMA) and the B block is polystyrene (PS) at a temperature of about 170 °C, as has been used in several experiments. Other constitutive relations can be considered.[20]

When a field is applied on a melt in the lamellar or hexagonal phases, it exerts torque which causes sample rotation. The torque is zero, and the energy lowest, when the lamellae or cylinders are oriented parallel to the field. In such states, as well as the disordered phase, the electrostatic energy, eq 3, of the system is equal to a reference energy, given below. The bcc array of spheres, on the other hand, always has dielectric interfaces that are not parallel to the field, and its electrostatic energy is higher than the reference value. Hence, the spheres elongate in the applied field direction, to an extent which is a balance between electrostatic and elastic forces, as calculated below.

The reference energy per polymer chain, in units of $k_B T$, is simply $-1/2\langle\kappa\rangle\hat{E}_0^2$, where $\hat{E}_0$ is the dimensionless applied field, the physical field expressed in natural unit $(k_B T/\epsilon_0 \upsilon_p)^{1/2}$

$$\hat{E}_0 = \left(\frac{\epsilon_0 \upsilon_p}{k_B T}\right)^{1/2} E_0 \quad (6)$$

Let us estimate the value of the actual applied field corresponding to $\hat{E}_0 = 1$. At 100 °C and using typical polymer volume per chain in the range $\upsilon_p \simeq 50-250$ nm³, we find $E_0 \simeq 47-107$ V/$\mu$m. This is a relatively large field that can cause dielectric breakdown in some BCP films. Therefore, the experimentally interesting regime is usually $\hat{E}_0 \lesssim 1$.

The free energy $F_{tot}$ as formulated above is valid close to the ODT point (weak segregation limit), where the concentration variations are small, $\phi(\mathbf{r}) \ll 1$, and therefore the analysis can be carried out within the so-called *one-mode approximation*. Motivated by recent experiments,[12,14] we concentrate on the transition from distorted spheres to cylinders or disordered melt in the presence of an applied electric field. Taking $\mathbf{E}_0$ to be in the (1,1,1) direction, we write the order parameter $\phi$ as a linear superposition of six components

$$\phi = w\phi_1 + g\phi_2 \quad (7)$$

where

$$\phi_1 = \sum_{i=1}^{3} \cos(\mathbf{q}_i \cdot \mathbf{r}), \quad \phi_2 = \sum_{i=1}^{3} \cos(\mathbf{k}_i \cdot \mathbf{r}) \quad (8)$$

The $q$'s and $k$'s are wavevectors given by

$$\mathbf{q}_1 = \frac{q_0}{\sqrt{2}}(-1,0,1), \quad \mathbf{q}_2 = \frac{q_0}{\sqrt{2}}(1,-1,0), \quad \mathbf{q}_3 = \frac{q_0}{\sqrt{2}}(0,1,-1)$$

$$\mathbf{k}_1 = \frac{q_0}{\sqrt{2}}(1,0,1), \quad \mathbf{k}_2 = \frac{q_0}{\sqrt{2}}(1,1,0), \quad \mathbf{k}_3 = \frac{q_0}{\sqrt{2}}(0,1,1) \quad (9)$$

and all have the same magnitude $q_0$. The three linearly dependent $\mathbf{q}_i$ are orthogonal to the (1,1,1) direction and describe a hexagonal phase with axis along that direction. The three $\mathbf{k}_i$ have equal and nonzero projections on the (1,1,1) axis. The six wavevectors transform into one another under the symmetry operations of the bcc phase. In the absence of an external field, each of these wavevectors would contribute equally in the order parameter expansion,[19] so that $g$ and $w$ would be equal. These wavevectors characterize the first mode in such an expansion. Hence the name of the approximation.

The amplitudes $w(E_0)$ and $g(E_0)$ depend on the magnitude of the average external field $E_0$. Depending on the values of the two amplitudes, $g$ and $w$, we can represent the order parameter of all phases of interest in the form of eq 7: $w = g \neq 0$ represents an undistorted bcc, while an $R\bar{3}m$ (distorted bcc) phase oriented along the (1,1,1) direction is represented by two nonzero amplitudes $w \neq g$. A hexagonal phase of cylinders whose long axis is in the (1,1,1) direction has $w \neq 0$ and $g = 0$. And finally, $g = w = 0$ represents the disordered melt. As was mentioned above, the spatially averaged electric field is simply the magnitude of the external field, $E_0$. However, local changes in $\phi(\mathbf{r})$ give rise to local changes in $\kappa(\mathbf{r})$. Consequently, the electric field can be written as follows:

$$\mathbf{E} = -\nabla\psi = \mathbf{E}_0 - \nabla\delta\psi \quad (10)$$

where $\delta\psi$ is the deviation of the potential from the average. With this representation of the field, the Maxwell equation, eq 4, becomes

$$\Delta\kappa\nabla\phi(\mathbf{r})\cdot\nabla\delta\psi(\mathbf{r}) + \Delta\kappa\phi(\mathbf{r})\nabla^2\delta\psi(\mathbf{r}) + \langle\kappa\rangle\nabla^2\delta\psi(\mathbf{r}) = \Delta\kappa\mathbf{E}_0\cdot\nabla\phi(\mathbf{r}) \quad (11)$$

It is clear that a necessary condition for a solution of this equation is that the behavior under any symmetry operations of the third term on the left-hand side must be the same as the behavior of the right-hand side; i.e., the symmetry of $\nabla^2\delta\psi(\mathbf{r})$ must be the same as that of $\mathbf{E}_0\cdot\nabla\phi(\mathbf{r})$. As the symmetry of the order parameter is known in any ordered phase, the symmetry of the potential is therefore determined. In particular, with $\mathbf{E}_0$ in the (1,1,1) direction and with the order parameter in the distorted bcc phase given in the one-mode approximation by eqs 7 and 8, one finds immediately that $\delta\psi(\mathbf{r})$ must take the form

$$\delta\psi(\mathbf{r}) = \frac{\beta E_0}{q_0}\sum_{i=1}^{3}\sin(\mathbf{k}_i\cdot\mathbf{r}) \quad (12)$$

where $\beta$ is to be determined. We now insert the $\mathbf{E}$-field expression of eq 10 into the electrostatic free energy, eq 3. Using the definitions of eqs 7−9 and the properties

$$\mathbf{q}_i\cdot(1,1,1) = 0; \quad |\mathbf{q}_i|^2 = q_0^2; \quad \mathbf{q}_i\cdot\mathbf{q}_j = -q_0^2/2, \quad i \neq j \quad (13)$$

and

$$\mathbf{k}_i\cdot(1,1,1) = 2q_0/\sqrt{2}; \quad |\mathbf{k}_i|^2 = q_0^2; \quad \mathbf{k}_i\cdot\mathbf{k}_j = q_0^2/2, \quad i \neq j$$

$$\sum_{i=1}^{3}\mathbf{k}_i = \frac{2q_0}{\sqrt{2}}(1,1,1); \quad \mathbf{k}_i\cdot\mathbf{q}_i = 0; \quad \mathbf{k}_i\cdot\mathbf{q}_j = \pm\frac{q_0^2}{2}, \quad i \neq j \quad (14)$$

we can perform the rather straightforward spatial averages of the various terms in the free energy, eq 3, and obtain

$$F_{\text{es}} = -\frac{1}{2}\frac{\hat{E}_0^2}{\Omega}\int\kappa(\mathbf{r})\left[\frac{\mathbf{E}(\mathbf{r})}{E_0}\right]^2 \mathrm{d}^3r$$

$$= -\frac{3}{4}\langle\kappa\rangle\beta^2\hat{E}_0^2 - \frac{3}{8}w\Delta\kappa\beta^2\hat{E}_0^2 + \sqrt{\frac{3}{2}}\beta g\Delta\kappa\hat{E}_0^2 - \frac{1}{2}\langle\kappa\rangle\hat{E}_0^2 \quad (15)$$

The last term is simply the reference energy which is common to all phases.

For a given state of $\phi$ (a given BCP morphology), which is determined by a given value of $w$ and $g$, the value of $\beta(w,g)$ is determined by the Maxwell equation, eq 11. This is equivalent to obtaining it by taking the variation of $F_{\text{es}}$ with respect to $\beta$. One obtains $\beta = \sqrt{2/3}g\Delta\kappa/(\langle\kappa\rangle + 1/2 w\Delta\kappa)$, so that $F_{\text{es}}$ is given by

$$F_{\text{es}} = \left[\frac{(\Delta\kappa)^2}{2\langle\kappa\rangle + w\Delta\kappa}g^2 - \frac{1}{2}\langle\kappa\rangle\right]\hat{E}_0^2 \quad (16)$$

It is instructive to compare this result with the perturbation expression used by Amundson, Helfand, and co-workers[5,6]

$$F_{\text{es}}^{\text{AH}} = \left[\frac{(\Delta\kappa)^2}{2\langle\kappa\rangle}g^2 - \frac{1}{2}\langle\kappa\rangle\right]\hat{E}_0^2 \quad (17)$$

a result which agrees only with the terms of order zero of the power series expansion in $w\Delta\kappa/(2\langle\kappa\rangle)$ of our expression. For the dielectric constants of interest to us, $w\Delta\kappa/(2\langle\kappa\rangle) \approx 0.5w$. As the magnitude of the parameter $w$ reflects the degree of segregation, as shown by eq 7, one sees that the perturbation result becomes poorer as the segregation increases.

The origin of the difference between eqs 16 and 17 is clearly seen from the Maxwell equation, eq 11. The perturbation scheme takes the potential $\delta\psi$ and the order parameter $\phi$ to be small and therefore, in lowest order, ignores the contribution of the first two terms on the left-hand side compared to the third. This implies that $\Delta\kappa\phi/\langle\kappa\rangle \ll 1$ or, equivalently from eq 5, $(\kappa - \langle\kappa\rangle)/\langle\kappa\rangle \ll 1$. Thus, the assumption is essentially that the fractional variation in the dielectric constant due to the ordering is small. Furthermore, these ignored terms are precisely the ones which couple the electric field created by the polarization charge of the system to its own order parameter. In contrast, we keep all terms in the Maxwell equation so that the free energy contains the effects of the deformation of the order parameter due to the field the sample itself produces. Another consequence of the use of lowest order perturbation theory is that it yields a free energy which is symmetric under the interchange of monomers A and B. It misses the breaking of this symmetry due to the application of the electric field which couples differently to the A and B blocks. This effect is manifest only when the free energy contains the contribution arising from the change in the order parameter due to the field produced by the sample itself. It would occur in higher order of perturbation theory.

We now employ the single-mode Ansatz $\phi = w\phi_1 + g\phi_2$ in eq 1 and finally obtain for the total free energy per polymer chain in units of $k_BT$ the result

$$F_{\text{tot}} = \frac{3}{4}\tau(w^2 + g^2) + \frac{1}{4}\lambda w(3g^2 + w^2) + \frac{15}{64}u(g^4 + 4g^2w^2 + w^4) + \left[\frac{(\Delta\kappa)^2}{2\langle\kappa\rangle + w\Delta\kappa}g^2 - \frac{1}{2}\langle\kappa\rangle\right]\hat{E}_0^2 \quad (18)$$

In the next section we minimize this energy with respect to $w$ and $g$ at a given dimensionless external field $\hat{E}_0$ and polymer architecture $f$, calculate the elongation the spheres of the bcc phase, and obtain the phase diagram.

### III. Results

As noted above, the functional form $\phi = w\phi_1 + g\phi_2$ allows us to describe a bcc array of spheres (for which $w = g \neq 0$), a distorted bcc phase ($w \neq g \neq 0$), a hexagonal array of cylinders ($w \neq 0$, but $g = 0$), and a disordered phase ($w = g = 0$). We
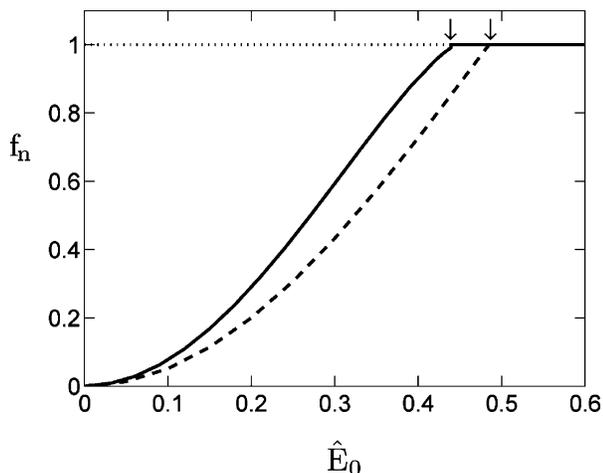
**Figure 1.** Normalized free energy per polymer chain $f_n$, defined in eq 19, of the distorted bcc phase ($R\bar{3}m$) as a function of dimensionless field $\hat{E}_0$. The system is characterized by $f = 0.3$ and $\chi N = 14.4$. We compare the one-mode calculation (solid line) as obtained from minimization of eq 18 with a SCF calculation (dashed line). The $R\bar{3}m$ phase in the SCF calculation has a lower free energy that the solid line (one mode) and crosses the hex energy at higher value of $\hat{E}_0$ of about 0.49, while the one-mode approximation crosses at $\hat{E}_0 \approx 0.43$ (both marked with arrows). In this figure and following ones we used $\kappa_A = 6$ and $\kappa_B = 2.5$, modeling a PMMA−PS copolymer.

are able, therefore, to obtain the full phase diagram by minimizing eq 18 with respect to the amplitudes $w$ and $g$.

Before presenting the phase diagram, let us consider a point in the $(f, N\chi)$ plane for which the stable phase at zero $E$ field has a bcc symmetry. For presentation purposes, in Figure 1 we have subtracted from the free energy the reference electrostatic energy, $-\langle\kappa\rangle\hat{E}_0^2/2$, common to all phases, also subtracted the total free energy of the bcc phase in zero field, $F_{\text{tot}}^{\text{bcc}}(0)$, and normalized the resulting free energy by that of the hex phase in zero field; that is, we have plotted

$$f_n \equiv \frac{F_{\text{tot}}(\hat{E}_0) + \langle\kappa\rangle\hat{E}_0^2/2 - F_{\text{tot}}^{\text{bcc}}(0)}{F_{\text{tot}}^{\text{hex}}(0)} \qquad (19)$$

In the figure we show how the free energy $f_n$ changes with $\hat{E}_0$ for $f = 0.3$ and $N\chi = 14.4$. At $\hat{E}_0 = 0$ the bcc is the stable phase, and its free energy increases with increasing field $\hat{E}_0$, until it equals the free energy of the hex phase at a transition field $\hat{E}_0 \simeq 0.43$. At larger fields the stable structure is a hex phase of cylinders oriented along the external field $\mathbf{E}_0$. The solid line in Figure 1 is the result obtained from the one-mode approximation given above, while the dashed line is obtained from the SCF theory (as in ref 15). It has a lower free energy. Consequently, the transition field in the SCF framework is higher and occurs at about $\hat{E}_0 \simeq 0.49$.

Figure 2 is a plot of the amplitudes $w(\hat{E}_0)$ and $g(\hat{E}_0)$, normalized by their zero-field value $w(\hat{E}_0{=}0) = g(\hat{E}_0{=}0)$. Both amplitudes start at their common value in the undistorted bcc phase. As the field increases, $w$ increases while $g$ decreases. The spheres elongate in the direction of the field as a result of competition between electrostatic and elastic forces. At the transition field, there is a sharp, discontinuous transition in the order parameter. Above this field, $w$ attains a fixed value while $g$ drops abruptly to zero. In this state the BCP morphology is that of cylinders oriented parallel to the external field. The dashed lines correspond to the values obtained from the SCF theory. Clearly, in the one-mode approximation, the spheres' deformation and eccentricity are larger than in the SCF theory.
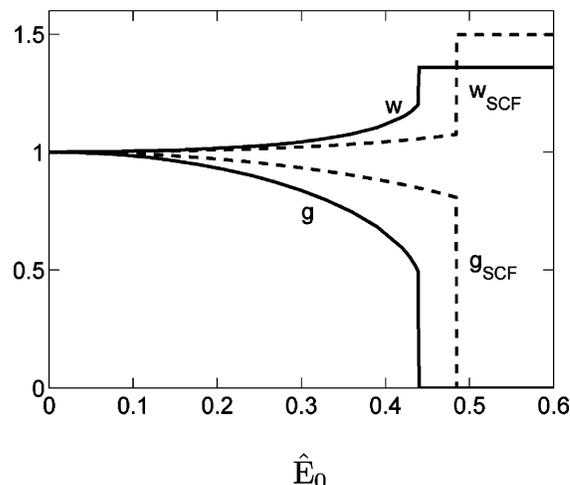


**Figure 2.** Amplitudes $w$ and $g$ normalized by their common value at zero $E$ field, $g(0) = w(0)$, as a function of dimensionless external field $\hat{E}_0$. Solid line: one-mode approximation. The amplitudes have a discontinuous jump at $\hat{E}_0 \simeq 0.43$, where the structure contains cylinders oriented along the field ($g = 0$). Dashed lines: the same, but taken from a multimode SCF calculation (ref 15) with a jump at higher $E$ values of $\hat{E}_0 \simeq 0.49$. All parameters as in Figure 1.
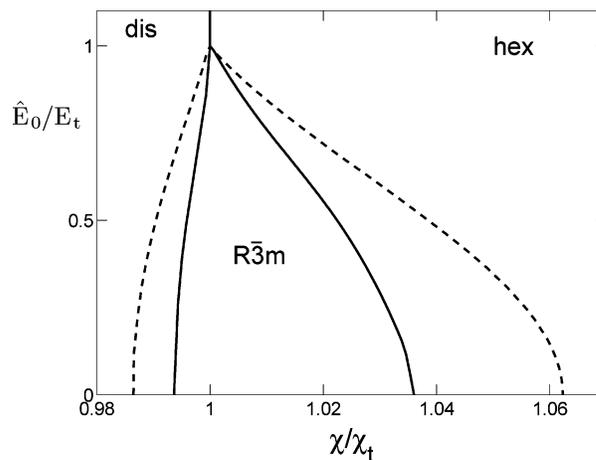


**Figure 3.** Phase diagram in the $(\chi/\chi_t, \hat{E}_0/E_t)$ rescaled plane for a fixed value of BCP asymmetry, $f = 0.3$. The distorted bcc ($R\bar{3}m$) region is confined between two transition lines which terminate at a triple point $(\chi_t, E_t)$. The other two phases are the disordered one (dis) and the hexagonal one (hex). The solid lines are the prediction of the one-mode approximation, with axes scaled by the appropriate $\chi_t \simeq 14.3/N$ and $E_t \simeq 0.49$. Dashed lines are the SCF calculation scaled by the appropriate SCF values of $\chi_t \simeq 14.11/N$ and $E_t \simeq 0.668$.

The above calculation can be repeated for any $(f, N\chi)$ and $\hat{E}_0$ field values and allows the construction of the full three-dimensional phase diagram in the $(f, N\chi, \hat{E}_0)$ parameter space. In Figure 3 we present a cut of the phase diagram at fixed $f = 0.3$. The region of a stable $R\bar{3}m$ phase (distorted bcc) is bound by two lines of phase transitions: one between this phase and the disordered phase and the other between it and the hex phase. These two lines meet at the triple point $(\chi_t, E_t)$. In Figure 3, the different triple point values obtained from the two calculations are used to rescale both axes: $\chi/\chi_t$ and $\hat{E}_0/E_t$. At fields larger than $E_t$, the $R\bar{3}m$ is not stable at any value of $\chi$. The solid lines in the figure are the one-mode prediction, while the dashed lines are obtained with the SCF calculation. The values of $E_t$ are 0.49 and 0.67 for the two theories, respectively. Were this phase diagram to be measured in a polymorphic system composed of grains of various orientations, the first-order transitions would not take place at a single temperature for a given field, but those in grains of different orientations would occur at different

temperatures, causing a blurring of the phase boundaries. In addition, because of long characteristic times associated with reorientation of grains, what is seen at the transition would depend on the observation time and sample history.

For an additional comparison between the theories, we have examined the case in which, at a fixed value of $f = 0.3$, the dielectric constants of the majority and minority components are interchanged (i.e., $\kappa_A = 6.0 \leftrightarrow \kappa_B = 2.5$, hence, $\Delta\kappa \rightarrow -\Delta\kappa$). In both theories we find an increase in the value of the external field needed to bring about a transition from the distorted bcc phase to the hex phase. Thus, this subtle effect, which is not captured by the perturbation result of eq 17, is obtained in the simple one-mode approximation, eq 16.

## IV. Conclusions

A simple theory for a nonhomogeneous diblock copolymer (BCP) melt in an external electric field is presented and compared with a more accurate, but more computationally intensive, self-consistent-field (SCF) one. The differences between the two theories in zero external field are well-known. In particular, the accuracy of the phase boundaries produced by the one-mode approximation deteriorates outside the vicinity of the ODT point (weak segregation) as compared to the SCF theory.[19] However, as in the zero field case, the qualitative behavior of the system in the presence of a field is described surprisingly well. The simple one-mode approximation captures the elongation of the spheres of a bcc phase when placed under an external field. The elongation is in the direction of the applied $E_0$ field. The two amplitudes describing this elongation, $w$ and $g$, are shown in Figure 2. At a threshold value of the electric field, a first-order transition to a hexagonal phase occurs and the amplitudes jump discontinuously.

As shown in Figure 3, the simple, analytic, one-mode approximation also captures the essence of the phase diagram: the reduction in the phase space occupied by the distorted bcc phase as the field increases and its eventual disappearance at a triple point.

The full electrostatic free energy contribution is included consistent within the one-mode approximation, eq 16, in contrast to previous analytical studies,[5,6,12,14] in which only quadratic terms in the electrostatic potential were retained. As a consequence, the theory captures the subtle interplay between structure and electrostatic response as evidenced by its prediction of a different critical field for phase transitions when the dielectric

constants of the constituents are interchanged, a prediction in agreement with the more accurate theory.[15]

Given its ability to capture all of the above effects and given its extreme simplicity, such a theory could serve for useful exploratory studies in other problems concerning the effect of electric fields on block copolymers.

## References and Notes

(1) Hart, S. D.; Maskaly, G. R.; Temelkuran, B.; Prideaux, P. H.; Joannopoulos, J. D.; Fink, Y. *Science* **2002**, *296*, 510.
(2) Pernot, H.; Baumet, M.; Court, F.; Leibler, L. *Nat. Mater.* **2002**, *1*, 54.
(3) Ruzette, A. V.; Leibler, L. *Nat. Mater.* **2005**, *4*, 19.
(4) Thurn-Albrecht, T.; Schotter, J.; Kästle, G. A.; Emley, N.; Shibauchi, T.; Krusin-Elbaum, L.; Guarini, K.; Black, C. T.; Tuominen, M. T.; Russell, T. P. *Science* **2000**, *290*, 2126.
(5) Amundson, K.; Helfand, E.; Quan, X.; Smith, S. D. *Macromolecules* **1993**, *26*, 2698.
(6) Amundson, K.; Helfand, E.; Quan, X.; Hudson, S. D.; Smith, S. D. *Macromolecules* **1994**, *27*, 6559.
(7) Pereira, G. G.; Williams, D. R. M. *Macromolecules* **1999**, *32*, 8115.
(8) Thurn-Albrecht, T.; DeRouchey, J.; Russell, T. P. *Macromolecules* **2000**, *33*, 3250.
(9) Ashok, B.; Muthukumar, M.; Russell, T. P. *J. Chem. Phys.* **2001**, *115*, 1559.
(10) Onuki, A.; Fukuda, J. *Macromolecules* **1995**, *28*, 8788.
(11) Tsori, Y.; Andelman, D. *Macromolecules* **2002**, *35*, 5161.
(12) Tsori, Y.; Tournilhac, F.; Andelman, D.; Leibler, L. *Phys. Rev. Lett.* **2003**, *90*, 145504.
(13) Tsori, Y.; Tournilhac, F.; Leibler, L. *Macromolecules* **2003**, *36*, 5873.
(14) Xu, T.; Zvelindovsky, A. V.; Sevink, G. J. A.; Gang, O.; Ocko, B.; Zhu, Y.; Gido, S. P.; Russell, T. P. *Macromolecules* **2004**, *37*, 6980.
(15) Lin, C.-Y.; Schick, M.; Andelman, D. *Macromolecules* **2005**, *38*, 5766.
(16) Leibler, L. *Macromolecules* **1980**, *13*, 1602.
(17) Ohta, T.; Kawasaki, K. *Macromolecules* **1986**, *19*, 2621.
(18) Fredrickson, G. H.; Helfand, E. *J. Chem. Phys.* **1987**, *87*, 697.
(19) Matsen, M. W.; Schick, M. *Phys. Rev. Lett.* **1994**, *72*, 2660.
(20) We briefly mention that a quadratic constitutive relation between $\epsilon$ and $\phi$, $\epsilon = \epsilon^{(0)} + \epsilon^{(1)}\phi + \epsilon^{(2)}\phi^2$, was previously investigated in refs 5, 6, and 21. The existence of the quadratic term leads to an upward shift in the ODT temperature: $\Delta T_{ODT} = v_p \epsilon^{(2)}/k_B E_0^2$, where $v_p$ is the volume of one BCP chain. This shift is typically small.
(21) Tsori, Y.; Tournilhac, F.; Leibler, L. *Nature (London)* **2004**, *430*, 544.